THE JOURNAL OF PHYSICAL CHEMISTRY Letters

LETTER

pubs.acs.org/JPCL

Defocused Emission Patterns from Chiral Fluorophores: Application to Chiral Axis Orientation Determination

A. Cyphersmith, A. Maksov, R. Hassey-Paradise,[†] K. D. McCarthy,[‡] and M. D. Barnes*

Department of Chemistry and Department of Physics, University of Massachusetts Amherst, 710 North Pleasant Street, Amherst, Massachusetts 01003, United States

ABSTRACT: Experimental defocused fluorescence emission patterns from single chiral molecular systems are compared to semiclassical simulations as a means for a priori determination of chiral axis orientation in single-molecule systems. Using a coupled-oscillator model as a radiation source, we show that the basic features of defocused emission patterns from chiral fluorophores can be recovered and suggests the feasibility of chiral axis orientation determination (within some limits) in single-molecule systems.

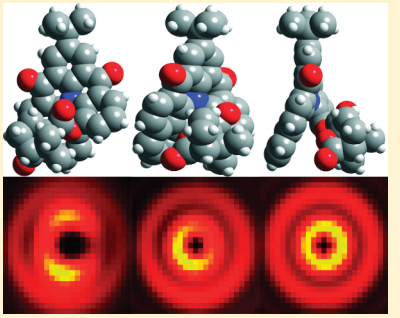

SECTION: Nanoparticles and Nanostructures

Understanding the orientational dependence of molecular chiroptical response is the key to next-generation photonic devices operating on circular polarization states[1−4] and explaining chiroptical responses from achiral sources, such as water.[5] Additionally, understanding the effects of solvation and local dielectric environment[6−8] on chiroptical response is greatly complicated by the entanglement with orientation.[9,10] In dye-doped crystals[11,12] and molecular systems immobilized at a surface, orientational contributions, related to off-diagonal elements of the rotatory strength tensor, can dominate the measured chiroptical dissymmetry. Thus, a great deal of experimental effort has been focused recently on experimental probes of molecular chirality in systems with well-defined orientation. Single-molecule spectroscopy provides an opportunity to probe these heterogeneities; however, in order to disentangle orientational and dielectric contributions to the net chiral dissymmetry, it is critical to develop tools enabling nondestructive orientation determination independent of the chiral dissymmetry measurement. In this Letter, we describe an adaptation of the method of defocused emission pattern imaging to the problem of orientation determination of single chiral fluorophores immobilized at a surface. We show that simulations using a coupled-oscillator model[13−15] as an electrodynamic source recover the qualitative features of experimentally observed defocused emission patterns from single (chiral) helicene molecules. Interesting similarities and differences with respect to 2D degenerate dipole systems (quantum dots) in terms of observed spatial asymmetry are discussed. These results demonstrate the feasibility of defocusing techniques for determining chiral axis orientation in the laboratory frame.

Emission pattern imaging of single-molecule fluorescence with a defocusing depth on the order of 1−2 optical wavelengths (500−1000 nm) has become a well-established technique for probing transition dipole orientation of molecular species in condensed phases.[16,17] For molecules having a single dominant transition moment component polarized along a body-fixed axis, the introduction of a small optical phase aberration (achieved through defocusing of the objective) reveals distinct spatial intensity patterns characteristic of linear "antenna"-like behavior.[16−22] Orientation information (specifically the two Euler angles that describe the antenna orientation in the laboratory frame) is typically obtained by matching the experimental image with a simulation and fitting procedure. Recently, defocused emission pattern techniques have been applied to quantum dot systems to reveal information on quasi-degenerate circular transition moments[23,24] and the orientation of the hexagonal symmetry axis of individual quantum dots. In this Letter, we examine the problem of chiral axis determination of single chiral molecules using similar radiation pattern imaging methodologies.

As has been demonstrated previously, calculations of circularly polarized emission anisotropy involving the rotatory strength tensor[25] of helicene molecules predict a significant contribution from the electric quadrupole transition moment, a contribution that is averaged away for rotating molecules. These calculations predict a distinct absorption and emission anisotropy that is dependent on molecular orientation. Future studies hoping to investigate the connection between molecular orientation and observed chiroptical properties will need a way of confirming molecular orientation. Success with determining the molecular orientation of linear molecules and CdSe quantum dots via defocused emission pattern imaging led us to consider using this method for determining the molecular orientation of chiral molecules. Our previous work[26] has shown that experimentally measured defocused emission patterns from single helicene molecules[27] are qualitatively different from linear dipole systems

Received: January 21, 2011
Accepted: February 23, 2011
Published: March 03, 2011

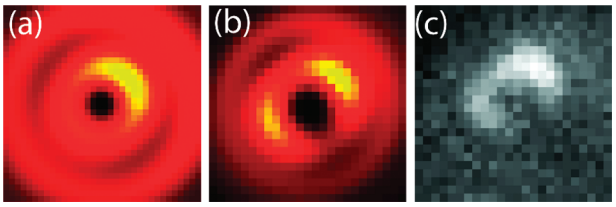

Figure 1. (a) Simulation from a 2D-DD model. For the c axis, an inclination angle of 60° and a polar angle of 60° were used. In this case, $\mu_2 = \mu_1$, and the dipoles are added incoherently. (b) An asymmetric emission pattern based on a coupled oscillator model. In this case, the two dipoles are added coherently and the parameters are $\Delta\theta = -10°$, $\Delta\varphi = 120°$, and $\mu_2/\mu_1 = 0.4$ with chiral axis Euler angles of $\theta = 0°$ and $\varphi = 210°$. (c) Experimental defocused emission pattern of a single helicene.

and the "2D-degenerate dipole" (2D-DD) patterns seen for quantum dots.[28] Quantum dot emission patterns can be modeled approximately as an incoherent superposition of electron−hole recombination transitions with left and right circular polarization. The defocused emission patterns from single QDs generally display bilateral symmetry, a symmetry that is independent of the hexagonal symmetry (c) axis orientation.

Figure 1 shows a comparison of two simulations in which (a) the two transition dipoles are degenerate and coplanar (2D-DD) and (b) in which a noncoplanarity of the dipoles is enforced by a spatial phase-difference between the two dipoles. Figure 1c shows a typical experimental defocused emission pattern from a single helicene molecule showing a characteristic spatial asymmetry. For simulations, differences in inclination angle between dipoles ($\Delta\theta$), differences in azimuthal angle between dipoles ($\Delta\varphi$), relative dipole magnitudes (μ_2/μ_1, where μ_1 is the strength of the first oscillator and μ_2 is the strength of the second oscillator), and chiral axis Euler angles are all considered. To match experimental conditions, a defocus depth of 700 nm, numerical aperture of 1.4, magnification of 400, and pixel area of 25 × 25 pixels was used for all simulations discussed here. On the basis of these parameters from the coupled oscillator model, we have matched defocused emission patterns of bridged triarylamines (helicenes) to simulated emission patterns. Figure 1 parts (b) and (c) show a qualitative fit between an experimentally observed defocused emission pattern from a chiral source (M2) and a simulated defocused image. The simulated image, Figure 1b, with parameters $\Delta\theta = -10°$, $\Delta\varphi = 120°$, and $\mu_2/\mu_1 = 0.4$, and chiral axis Euler angles of $\theta = 0°$ and $\varphi = 210°$ produced a qualitatively similar emission pattern to the one observed for this particular M2 helicene molecule. From the comparison in Figure 1, it is apparent that the coupled oscillator model successfully mimics the emission patterns from an inherently chiral source.

Asymmetric emission patterns[29,30] from individual quantum dots have been observed as well, which can be attributed to structural defects that break the symmetry of the left circularly polarized and right circularly polarized transitions, resulting in a net ellipticity in the fluorescence emission. For single (chiral) helicene molecules,[26,31] the defocused emission patterns show a significant distortion in the bilateral symmetry normally observed in emission patterns from achiral systems. Chiral chromophores such as triaryl amine helicenes have a transition moment possessing (in general) some finite electric quadrupole and magnetic dipole character. In principal, one can estimate the order of magnitude of these higher multipoles from measured chiroptical dissymmetries provided that the orientation is known.

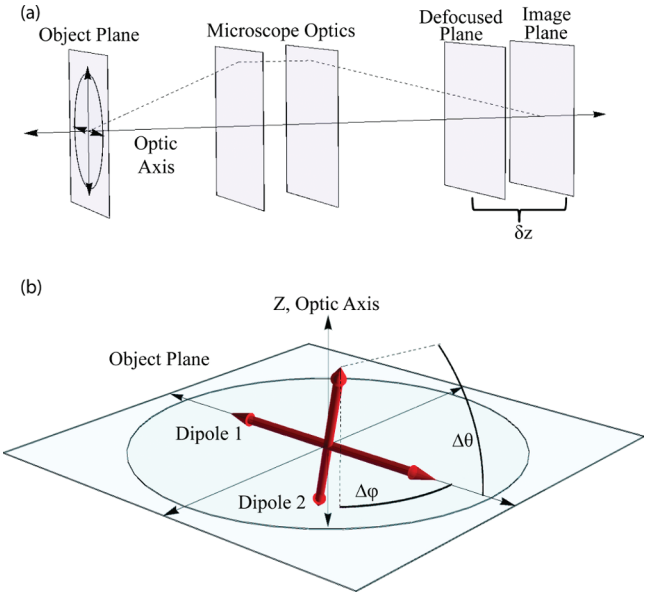

Figure 2. (a) Schematic of the relationship between the dipole source and the image projected onto the CCD camera. Note that δz is the defocusing depth. (b) Schematic of coupled oscillator in the object plane. Each dipole may be rotated in the polar (φ) angle and the inclination (θ) angle.

Here, we present a comparison of experimental results and computational simulation where the source radiation field was modeled as two coherently coupled noncoplanar one-dimensional electric dipoles, the Kirkwood model.[15] The Kirkwood model of a chiral system involves coherent coupling of two achiral systems (linear dipoles). In order to generate a chiral response, the two dipoles must be noncoplanar. In the simulations, we mimic this distance between dipoles as a phase shift; while the model shows two coplanar dipoles, it is emulating two noncoplanar dipoles through use of the phase shift. We find that the resulting simulated defocused images yield emission patterns similar to experimental observations on single chiral molecules and quantum dots showing strong ellipticity in fluorescence emission. Such a combination of dipoles allows the defocused emission patterns to be fit to three adjustable parameters corresponding to physical properties of the individual oscillators (i.e., dipole strength and orientation) and the two Euler angles of the chiral axis.

Figure 2 shows a schematic of the geometry used in our numerical simulations. The chiral electrodynamic source is based on a coupled-oscillator model of optical activity that parametrizes the optical response of an inherently chiral fluorophore in terms of two or more transition dipoles.[32] Our simulations are based on a formulation similar to the one that Bohmer and Enderlein[17,33] used to simulate emission patterns from 2D-DD systems. In recent work, we used a similar model to describe the incoherent superposition of 2 or 3 linear dipoles as a source to model the emission patterns of semiconductor CdSe/ZnS quantum dots and successfully applied this model to explain experimentally observed emission patterns and polarization properties. The transition from quantum dots to chiral molecules involves coherent coupling of the two main transition moments (which are incoherent superpositions in quantum dots) and enforcing a noncoplanarity in the transition dipole components (via a phase shift) to account for the circular dissymmetry. Each dipole

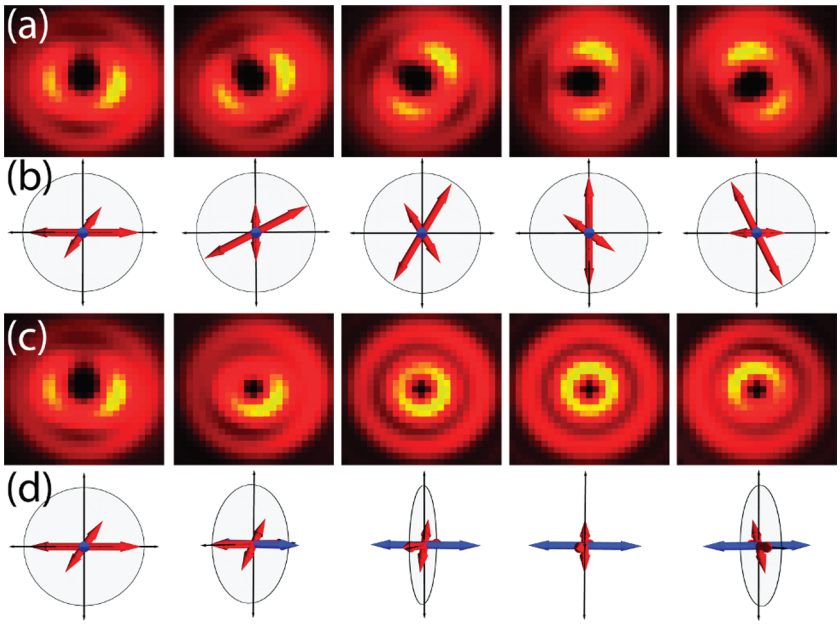

Figure 3. Effects of chiral axis orientation on simulated emission patterns. (a) Rotation of the chiral axis along azimuthal angles (φ) from 0 to 120° in steps of 30°. Note that the chiral axis remains fixed along the optic axis. (b) Illustration of the dipole configuration used to generate the corresponding emission pattern in (a). The dipoles are red, and the chiral axis is blue. (c) Rotation of the chiral axis along inclination angles (θ) from 0 to 120° in steps of 30°. Note that the chiral axis rotates away from the optic axis. For all images, the parameters $\Delta\theta = -10°$, $\Delta\varphi = 120°$, $\mu_2/\mu_1 = 0.4$, $\xi = -\pi/2$, and $\delta z = 700$ nm were used. (d) Illustration of the dipole configuration used to generate the corresponding emission pattern in (c). The dipoles are red, and the chiral axis is blue.

component was assigned two (s and p) unit vectors characterized by a specified azimuthal (θ) and polar (φ) angle. Emission patterns were simulated by integrating the Poynting flux from the electric and magnetic fields.

Instead of adding the Poynting vectors of each dipole source, as in the 2D-DD case, a phase factor was incorporated into the addition of the electric and magnetic fields.

$$\begin{aligned}\mathbf{E} &= E_1{}^{\mathrm{s}} \cos\theta_1 + E_1{}^{\mathrm{p}} \sin\theta_1 + \mathrm{e}^{-\mathrm{i}\xi}(E_2{}^{\mathrm{s}} \cos\theta_2 + E_2{}^{\mathrm{p}} \sin\theta_2)\\ \mathbf{B} &= B_1{}^{\mathrm{s}} \cos\theta_1 + B_1{}^{\mathrm{p}} \sin\theta_1 + \mathrm{e}^{-\mathrm{i}\xi}(B_2{}^{\mathrm{s}} \cos\theta_2 + B_2{}^{\mathrm{p}} \sin\theta_2)\end{aligned} \quad (1)$$

where s and p refer to the polarization states parallel to the glass interface of the microscope and the number specifies a particular dipole; an imaginary phase shift, ξ, is applied to dipole 2. The justification for the prescription in eq 1 is that it represents a simple way in which to mimic the net ensemble polarization of photons emitted by the chiral fluorophore; in essence, the second dipole, if given a phase factor of $\xi = -\pi/2$, would approximate the fields radiated by the effective magnetic dipole and electric quadrupole transition moments of the radiating system. Note that in the model presented here, the two dipoles share a common center, and this phase shift effectively approximates a displacement between the two dipoles.

A prominent feature of the chiral emission patterns in Figure 1b is the lack of bilateral symmetry, which recreates very well the observed emission patterns from a chiral molecule. The chiral emission patterns also appear tilted off axis when compared to the 2D-DD simulation; this is due to the combination of the phase shift and differing polar angles of the two dipoles. Figure 3 demonstrates the effect of rotation of the chiral axis through both inclination and azimuthal angles; as shown in Figure 2, the chiral axis is orthogonal to dipole 1 and lies along the optical axis for $\theta = 0°$. For some orientations, the emission from a coupled-oscillator source is qualitatively similar to the emission patterns observed in CdSe—ZnS quantum dots. Figure 3 also shows the orientation of the dipoles used in the simulation and the respective emission patterns. From this comparison of emission patterns and dipoles, it is apparent that the symmetry breaking occurs when the chiral axis lies along the optic axis.

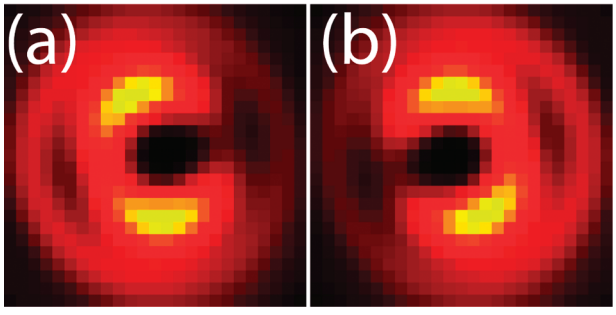

Figure 4. Comparison of simulations with identical relative orientations between dipoles. The azimuthal orientation of the chiral axis is 120° in (a) and 300° in (b).

As with emission patterns from CdSe/ZnS quantum dots, the signal-to-noise of the defocused images was lower when compared to in focus images due to the dispersion of photons over a larger area. The helicenes' signal-to-noise was lowered even further due to faster photobleaching times and an overall smaller signal budget. The number of fitting parameters resulted in ambiguity when matching experimental emission patterns. As shown in Figure 4, rotation around the chiral axis resulted in mirrored emission patterns, thus allowing either the chiral axis azimuthal angle or $\Delta\varphi$ to be adjusted in order to obtain a reasonable fit.

dx.doi.org/10.1021/jz2001024 |J. Phys. Chem. Lett. 2011, 2, 661–665

Our simulations of defocused emission patterns from chiral fluorophores recover the spatial asymmetry in observed defocused emission patterns from bridged triarylamine (helicene) molecules. There are obvious difficulties in unambiguous assignment of orientation angles, which derive from the finite spatial (k) resolution, the signal-to-noise ratio in the experimental measurements and the number of adjustable parameters used in the simulation. The assignment of Euler angles to both the chiral axis and individual dipole oscillators leads to (in some cases) a defocused emission pattern that is not unique with respect to more than one set of parameters, necessarily leading to uncertainty in orientation assignment of the chiral axis of the molecule. In addition, as observed in quantum dot systems,[34] the simulated defocused emission patterns are quite sensitive to the choice of model of the electrodynamic source. The basic features of experimentally observed defocused emission patterns for chiral molecules are similar to those of quantum dots, but with significant deviations that may provide clues as to relative strengths of the electric dipole and quadrupole character.

In principle, defocused emission patterns can be used to assign molecular orientations to individual chiral molecules in much the same way that they can currently be used to assign crystal axis orientations in CdSe−ZnS quantum dots. This Letter describes a complication that arises in the case of a chiral source and describes the observed asymmetry in terms of a coupled-oscillator molecule. In order to establish a more robust explanation of when this asymmetry occurs, it will be necessary to determine the dipole magnitude and orientation through another measurement, perhaps polarization, in addition to observing the emission patterns.

It may be possible, in future studies, to measure the ellipticity (linear anisotropy) of a chiral molecule in addition to obtaining an emission pattern. For a linear molecule such as DiIC18, the ellipticity would give a very clear picture of the molecular orientation. In the case of a coupled oscillator, the correlation between orientation and ellipticity is much less obvious. The ellpiticity would be an effect of the net projection of the two dipoles along the optic axis. Elipticity may be a useful parameter to measure in order to establish the ratio μ_2/μ_1 and may be a useful quantity to measure in future experiments.

We are currently investigating defocused emission patterns from surface-tethered helicenes (which constrain the molecular orientations), thus providing additional information to further refine the model. This would reduce the parameter space considerably and allow us to establish a quantitative connection between the coupled oscillator and the inherently chiral fluorophore model.

EXPERIMENTAL METHODS

Measurements were made with an inverted microscope and a 1.4 numerical aperture (NA) objective in a wide field setup. Samples of bridged triarylamines (M2 isomer) in a Zeonex matrix were prepared by drop casting a dilute solution (10^{-9} M) in cyclohexane and Zeonex onto a glass coverslip. The sample was illuminated with 30 μW of right circularly polarized light from the 457 nm line of a CW argon ion laser over an area with a 15 μm diameter. A XF2027 dichroic filter from Omega Optical was used with a 480 nm long-pass filter to block residual laser light. Defocused emission patterns were obtained by reducing the distance between the objective and sample by 700−900 nm via a servo-controlled microscope stage. Images were collected on a Princeton Instruments PhotonMax CCD (charged-coupled device) camera. Defocused emission pattern images were made by collecting about 2×10^6 photon counts over a 50 s exposure. In image space, the emission pattern is distributed over an area of about 20×20 pixels (with pixel dimensions of $16\,\mu\text{m} \times 16\,\mu\text{m}$). Blinking events occurred on the order of 1 ms to 1s and do not appear to have affected the observed defocused emission patterns.

AUTHOR INFORMATION

Present Addresses

[†]Department of Chemistry, New York University, New York City, NY.

[‡]Raytheon Corporation, Andover MA.

ACKNOWLEDGMENT

Support from the National Science Foundation (CHE-0848596) is gratefully acknowledged. M.D.B. acknowledges support as part of the Polymer-Based Materials for Harvesting Solar Energy (PHaSE), an Energy Frontier Research Center funded by the U.S. Department of Energy, Office of Science, Basic Energy Sciences, under Award Number DE-SC0001087.

REFERENCES

(1) Chen, S. H.; Katsis, D.; Schmid, A. W.; Mastrangelo, J. C.; Tsutsui, T.; Blanton., T. N. Circularly Polarized Light Generated by Photoexcitation of Luminophores in Glassy Liquid−Crystal Films. *Nature* **1999**, *397*, 506–508.

(2) Jeong, S. M.; Ha, N. Y.; Takezoe, H.; Nishimura, S.; Suzaki., G. Polarization-Tunable Electroluminescence Using Phase Retardation Based on Photonic Bandgap Liquid Crystal. *J. Appl. Phys.* **2008**, *103*, 113101.

(3) Wang, C. T.; Lin., T. H. Polarization-Tunable Chiral Nematic Liquid Crystal Lasing. *J. Appl. Phys.* **2010**, *107*, 123102.

(4) Yamaguchi, T.; Inagawa, T.; Nakazumi, H.; Irie, S.; Irie., M. Photoswitching of Helical Twisting Power of a Chiral Diarylethene Dopant: Pitch Change in a Chiral Nematic Liquid Crystal. *Chem. Mater.* **2000**, *12*, 869–871.

(5) Isborn, C.; Claborn, K.; Kahr., B. The Optical Rotatory Power of Water. *J. Phys. Chem. A* **2007**, *111*, 7800–7804.

(6) Wilson, S. M.; Wiberg, K. B.; Murphy, M. J.; Vaccaro., P. H. The Effects of Conformation and Solvation on Optical Rotation: Substituted Epoxides. *Chirality* **2008**, *20*, 357–369.

(7) Muller, T.; Wiberg, K. B.; Vaccaro., P. H. Cavity Ring-down Polarimetry (CRDP): A New Scheme for Probing Circular Birefringence and Circular Dichroism in the Gas Phase. *J. Phys. Chem. A* **2000**, *104*, 5959–5968.

(8) Kongsted, J.; Pedersen, T. B.; Osted, A.; Hansen, A. E.; Mikkelsen, K. V.; Christiansen., O. Solvent Effects on Rotatory Strength Tensors. 1. Theory and Application of the Combined Coupled Cluster/Dielectric Continuum Model. *J. Phys. Chem. A* **2004**, *108*, 3632–3641.

(9) Pedersen, T. B.; Hansen., A. E. Ab-Initio Calculation and Display of the Rotatory Strength Tensor in the Random-Phase-Approximation — Method and Model Studies. *Chem. Phys. Lett.* **1995**, *246*, 1–8.

(10) Autschbach, J.; Ziegler, T.; van Gisbergen, S. J. A.; Baerends., E. J. Chiroptical Properties from Time-Dependent Density Functional Theory. I. Circular Dichroism Spectra of Organic Molecules. *J. Chem. Phys.* **2002**, *116*, 6930–6940.

(11) Bing, Y. H.; Selassie, D.; Paradise, R. H.; Isborn, C.; Kramer, N.; Sadilek, M.; Kaminsky, W.; Kahr., B. Circular Dichroism Tensor of a Triarylmethyl Propeller in Sodium Chlorate Crystals. *J. Am. Chem. Soc.* **2010**, *132*, 7454–7465.

(12) Kaminsky, W.; Claborn, K.; Kahr., B. Polarimetric Imaging of Crystals. *Chem. Soc. Rev.* **2004**, *33*, 514–525.

(13) Fitts, D. D.; Kirkwood., J. G. The Theoretical Optical Rotation of Phenanthro[3,4-C]Phenanthrene. *J. Am. Chem. Soc.* **1955**, *77*, 4940–4941.
(14) Kirkwood., J. G. On the Theory of Optical Rotatory Power. *J. Chem. Phys.* **1937**, *5*, 479–491.
(15) L. D. Barron. *Molecular Light Scattering and Optical Activity*; Cambridge University Press: New York, 2004.
(16) Bartko, A. P.; Dickson., R. M. Three-Dimensional Orientations of Polymer-Bound Single Molecules. *J. Phys. Chem. B* **1999**, *103*, 3053–3056.
(17) Bohmer, M.; Enderlein., J. Orientation Imaging of Single Molecules by Wide-Field Epifluorescence Microscopy. *J. Opt. Soc. Am. B* **2003**, *20*, 554–559.
(18) Chung, I. H.; Shimizu, K. T.; Bawendi., M. G. Room Temperature Measurements of the 3D Orientation of Single CdSe Quantum Dots Using Polarization Microscopy. *Proc. Natl. Acad. Sci. U.S.A.* **2003**, *100*, 405–408.
(19) Bartko, A. P.; Dickson., R. M. Imaging Three-Dimensional Single Molecule Orientations. *J. Phys. Chem. B* **1999**, *103*, 11237–11241.
(20) Lieb, M. A.; Zavislan, J. M.; Novotny., L. Single-Molecule Orientations Determined by Direct Emission Pattern Imaging. *J. Opt. Soc. Am. B* **2004**, *21*, 1210–1215.
(21) Brokmann, X.; Ehrensperger, M. V.; Hermier, J. P.; Triller, A.; Dahan., M. Orientational Imaging and Tracking of Single Cdse Nanocrystals by Defocused Microscopy. *Chem. Phys. Lett.* **2005**, *406*, 210–214.
(22) Mattheyses, A. L.; Axelrod., D. Fluorescence Emission Patterns near Glass and Metal-Coated Surfaces Investigated with Back Focal Plane Imaging. *J. Biomed. Opt.* **2005**, *10*, 054007.
(23) Efros., A. L. Luminescence Polarization of CdSe Microcrystals. *Phys. Rev. B* **1992**, *46*, 7448–7458.
(24) Htoon, H.; Crooker, S. A.; Furis, M.; Jeong, S.; Efros, A. L.; Klimov., V. I. Anomalous Circular Polarization of Photoluminescence Spectra of Individual CdSe Nanocrystals in an Applied Magnetic Field. *Phys. Rev. Lett.* **2009**, *102*, 017402.
(25) Nina Berova, K. N., Robert, W.W. *Circular Dichroism: Principles and Applications.*; Wiley: New York, 2000.
(26) Hassey, R.; Swain, E. J.; Hammer, N. I.; Venkataraman, D.; Barnes., M. D. Probing the Chiroptical Response of a Single Molecule. *Science* **2006**, *314*, 1437–1439.
(27) Field, J. E.; Hill, T. J.; Venkataraman., D. Bridged Triarylamines: A New Class of Heterohelicenes. *J. Org. Chem.* **2003**, *68*, 6071–6078.
(28) Brokmann, X.; Coolen, L.; Hermier, J. P.; Dahan., M. Emission Properties of Single CdSe/ZnS Quantum Dots Close to a Dielectric Interface. *Chem. Phys.* **2005**, *318*, 91–98.
(29) Schuster, R.; Barth, M.; Gruber, A.; Cichos., F. Defocused Wide Field Fluorescence Imaging of Single CdSe/ZnS Quantum Dots. *Chem. Phys. Lett.* **2005**, *413*, 280–283.
(30) Patra, D.; Gregor, I.; Enderlein, J.; Sauer., M. Defocused Imaging of Quantum-Dot Angular Distribution of Radiation. *Appl. Phys. Lett.* **2005**, *87*, 101103.
(31) Hassey-Paradise, R.; Cyphersmith, A.; Tilley, A. M.; Mortsolf, T.; Basak, D.; Venkataraman, D.; Barnes., M. D. Dissymmetries in Fluorescence Excitation and Emission from Single Chiral Molecules. *Chirality* **2010**, *21*, E265–E276.
(32) T. T. D.P. Craig. *Molecular Quantum Electrodynamics*; Academic Press: New York, 1984.
(33) Patra, D.; Gregor, I.; Enderlein., J. Image Analysis of Defocused Single-Molecule Images for Three-Dimensional Molecule Orientation Studies. *J. Phys. Chem. A* **2004**, *108*, 6836–6841.
(34) Cyphersmith, A.; Early, K.; Maksov, A.; Graham, J.; Wang, Y. K.; Barnes., M. Disentangling the Role of Linear Transition Dipole in Band-Edge Emission from Single CdSe/ZnS Quantum Dots: Combined Linear Anisotropy and Defocused Emission Pattern Imaging. *Appl. Phys. Lett.* **2010**, *97*, 121915.